Three-Dimensional Shear-Driven Boundary-Layer Flow with Streamwise Adverse Pressure Gradient

David M. Driver*
NASA Ames Research Center, Moffett Field, California
and
Sheshagiri K. Hebbar†
Naval Postgraduate School, Monterey, California

The effects of adverse pressure gradient on a three-dimensional turbulent boundary layer are studied in an axisymmetric forward-facing step geometry. Velocity measurements made using a three-component laser Doppler velocimeter include mean flow as well as Reynolds stresses and velocity triple-product correlations. Turbulent Prandtl mixing lengths are extracted from the data, showing the effects of curvature. Streamwise pressure gradient is seen to alter streamwise velocity and Reynolds stress without significantly affecting transverse velocity and Reynolds stress. Reynolds stresses are seen to respond slowly (lag) to changes in the mean flow strain rate.

Nomenclature

C_{f_x} = axial (streamwise) skin-friction coefficient, $=\tau_{w_x}/\frac{1}{2}\rho_o U_o^2$
C_{f_z} = circumferential (transverse) skin-friction coefficient, $=\tau_{w_z}/\frac{1}{2}\rho_o U_o^2$
C_p = pressure coefficient, $=(P-P_o)/\frac{1}{2}\rho_o U_o^2$
H = step height, $=2.54$ cm
k = turbulent kinetic energy, $=(\overline{u^2}+\overline{v^2}+\overline{w^2})/2$, assumed $\overline{w^2}=(\overline{u^2}+\overline{v^2})/2$, where $\overline{w^2}$ not measured
l = mixing length, $=\sqrt[4]{\overline{uv}^2+\overline{vw}^2}/\sqrt{(\partial U/\partial y)^2+(\partial W/\partial y - W/r)^2}$
P = static pressure
r = radial distance from centerline of cylinder
U_o = upstream freestream velocity (used in normalization of data), $=36.5$ m/s
U,V,W = mean velocity components in X, Y, and Z directions, respectively
u_τ = friction velocity, $=\sqrt{\tau_w/\rho_w}$
u,v,w = fluctuating velocity components in X, Y, and Z directions, respectively
$\overline{u^2},\overline{v^2},\overline{w^2}$ = mean-square velocity fluctuations in X, Y, and Z directions, respectively
$\overline{uv},\overline{vw},\overline{uw}$ = tubulent velocity fluctuation correlations
$\overline{u^3},\overline{uw^2}$, $\overline{uw^2},\overline{vu^2}$, $\overline{v^3},\overline{vw^2}$, $\overline{wu^2},\overline{wv^2}$, $\overline{w^3},\overline{uvw}$ = turbulent triple-velocity correlation, assumed $\overline{uw^2}=(\overline{u^3}+\overline{uv^2})/2$ and $\overline{vw^2}=(\overline{vu^2}+\overline{v^3})/2$, where $\overline{uw^2}$ and $\overline{vw^2}$ were not measured
$\overline{vk}$ = turbulent triple-velocity correlation, $=(\overline{vu^2}+\overline{v^3}+\overline{vw^2})/2$
W_s = transverse (circumferential) velocity on surface of rotating cylinder (spinning section), $=36.5$ m/s
X,Y,Z = coordinate system representing axial, normal, and circumferential distances from the downstream end of spinning cylinder (see Fig. 1)
δ = local boundary-layer thickness
ε = dissipation rate of kinetic energy
ν = molecular kinematic viscosity of air, $=0.000015$ m^2/s
ρ = air density, $=1.2$ kg/m^3
τ_w = total wall shear stress
τ_{w_x},τ_{w_z} = axial (streamwise) and circumferential (transverse) wall shear stresses, respectively

Subscripts

o = upstream freestream conditions at X, $=-12.7$ mm
w = wall conditions

Introduction

DIFFICULTY in predicting aerodynamic flows is often attributable to inaccuracies in turbulence modeling. While the exact equations of fluid flow are well known, these equations are difficult to solve when the flow becomes turbulent, due to difficulties in resolving all of the small-scale motion associated with turbulence. Alternatively, the exact equations of motion are simplified by time averaging them, resulting in a relatively few integral variables (Reynolds stresses). In so doing, information is lost, and additional equations (models) for the Reynolds stresses are needed to fill in the lost information due to averaging. Capturing the behavior of turbulence in these few variables is difficult, at best, as turbulence is highly sensitive to many different flow phenomena (strain rates), such as pressure gradient, crossflow, and curvature, to mention a few. Furthermore, combinations of different types of strain rates do not necessarily affect the turbulence in a simple way. Systematic experiments are needed to study the effects of extra rates of strain on turbulence and the associated models.

One of the most commonly encountered extra rates of strain is due to three-dimensional crossflow ($\partial W/\partial y \neq 0$).

Presented as Paper 88-3661 at the First National Fluid Dynamics Congress at Cincinnati, OH, July 25-28, 1988; received Sept. 19, 1988; revision received Jan. 30, 1989.

*Research Scientist.
†Adjunct Professor, Department of Aeronautics and Astronautics. Senior Member AIAA.

Here, experiments by Bradshaw and Pontikos[1] and Driver and Hebbar[2] indicate that crossflow tends to reduce the mixing (i.e., $\overline{uv}$ shear stress) in the boundary layer. In addition, Reynolds stresses are seen to respond slowly to changes in mean flow strain rate thereby creating difficulties for simple equilibrium turbulence models.

Another commonly encountered extra rate of strain is due to pressure gradient ($\partial U/\partial x \neq 0$). Adverse pressure gradient flows ($\partial U/\partial x < 0$), such as those of Simpson et al.,[3] tend to increase the turbulent mixing and $\overline{uv}$ shear stress in the middle portion of the boundary layer. However, this increased mixing or Reynolds stress takes time to develop and does not immediately respond to the changes in mean flow strain rate produced by the pressure gradient (often referred to as a lag phenomenon). Simple equilibrium turbulence models have difficulty predicting this lag phenomenon.

Flows often contain combinations of adverse pressure gradient and crossflow,[1,4-6] and they can be difficult to interpret without the ability to relax either or both effects independently. Johnston's[5] "swept, forward-facing step" flow most closely resembles the current flow. The Reynolds shear stresses in Johnston's flow were slow to respond to the mean flow strain rate (as in the previously mentioned flows), and they developed in a direction opposite to that of the mean flow strain rate.

Furuya et al.[7] produced mild streamwise pressure gradients on their spinning cylinder model and found that the transverse component of mean flow was relatively unaffected by the streamwise pressure gradient. No measurements of Reynolds stresses were reported.

In the present work, the effects of adverse pressure gradient on a three-dimensional turbulent boundary layer were studied in an axisymmetric forward-facing step geometry. This is an extension of work by Hebbar and Driver[8] in which surface skin friction and pressure measurements were presented for a series of forward-facing step geometries. Surface skin-friction measurements in the previous study suggested that crossflow was relatively insensitive to streamwise pressure gradient. In this work, mean flow and fluctuating quantities proved this to be true. This work was undertaken in order to test turbulence models.

Experiment

Test Configuration

The experiment was conducted in a 31 × 31-cm low-speed wind tunnel with a 14.0-cm-diam cylinder running the length of the tunnel along the tunnel centerline (Fig. 1). The tunnel walls were deflected to compensate for boundary-layer growth and produce zero pressure gradient. An upstream section of the cylinder (91.4-cm long) was made to rotate, thus producing a lateral flow in the boundary layer. A downstream section remained stationary. The gap between the spinning and stationary sections was closed to within 0.0254 cm, and the two cylinders were equal in diameter (14 cm) to within ±0.02 cm (the upstream spinning cylinder was slightly smaller in radius by 0.01 cm ($y^+ = 10$) than the stationary section).

A pressure gradient was introduced by mounting a circular sleeve on the stationary section acting as a forward-facing step 2.54-cm high. The forward-facing step was located 15.4-cm downstream of the junction between the spinning and stationary section (corresponding to $X/H = 6.06$) in an effort to locate the steep pressure rise on the stationary section just downstream of the cylinder's junction. By locating the step at $X = 15.4$ cm, the flow at the end of spin was relatively uncontaminated by pressure gradient, while immediately downstream the pressure gradient grows (a region where transverse flow is rapidly evolving). Measurements were performed primarily on the stationary sections where the boundary layer was relaxing from the sudden change in boundary conditions (cessation of spin). Here the combined effects of pressure gradient and transverse strain were studied.

Test conditions are based on an upstream reference velocity of 36.5 m/s and atmospheric pressure and temperature. Two cases were studied: one in which the spinning cylinder was made to rotate with a tangential velocity of 36.5 m/s, and a second case where the cylinder was held stationary. The boundary-layer thickness δ_o at the end of the spinning section was 2.8 cm with a momentum thickness Reynolds number Re_θ of 6.9×10^3. For the nonspinning case, $\delta_o = 1.8$ cm and $Re_\theta = 4.5 \times 10^3$.

Surface and Flowfield Measurements

Surface-flow measurements were reported in a previous study by Hebbar and Driver.[8] Coefficient of pressure (reproduced here for completeness) is believed to be accurate to ±0.005.

Flowfield measurements were made using a three-component laser Doppler velocimeter (LDV) to obtain three mean-flow components and all six Reynolds stresses (see Ref. 9 for a description). Flowfield measurements were complimented with a conventional two-component LDV in flow locations near the step where access by the three-component system was not possible. Uncertainties in U,V,W were estimated to be ±2%. Uncertainties in u^2, v^2, w^2 were estimated to be ±8, ±8, and ±15%, respectively, while uncertainties in $\overline{uw},\overline{uw},\overline{uw}$ were estimated to fall in the range of −10 to +25%. The weighted uncertainty reflects the general belief that shear stresses measured by the three-dimensional LDV are systematically low in the inner portion of the boundary layer because of multiple seed particles in the measurement volume (see Ref. 9 for a discussion). The uncertainties quoted here include the amount by which the stresses are believed to be low. Triple-product correlations (i.e., $\overline{vk}$) are also expected to be measured low by 10–20%, and uncertainties which include this bias are estimated to be −20 to +30%. the two-component LDV does not suffer from this complication and uncertainties in $\overline{uv}$ are ±10%.

Flowfield Quality

As reported by Hebbar and Driver,[8] the flowfield in the test section was of good quality with a pressure gradient that was

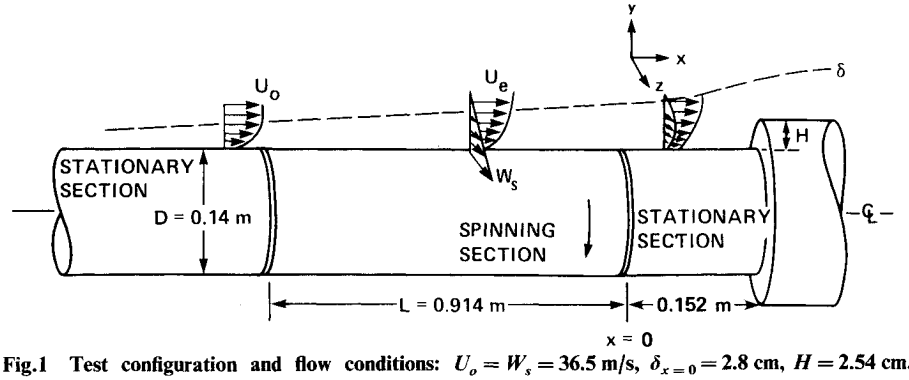

Fig.1 Test configuration and flow conditions: $U_o = W_s = 36.5$ m/s, $\delta_{x=0} = 2.8$ cm, $H = 2.54$ cm.

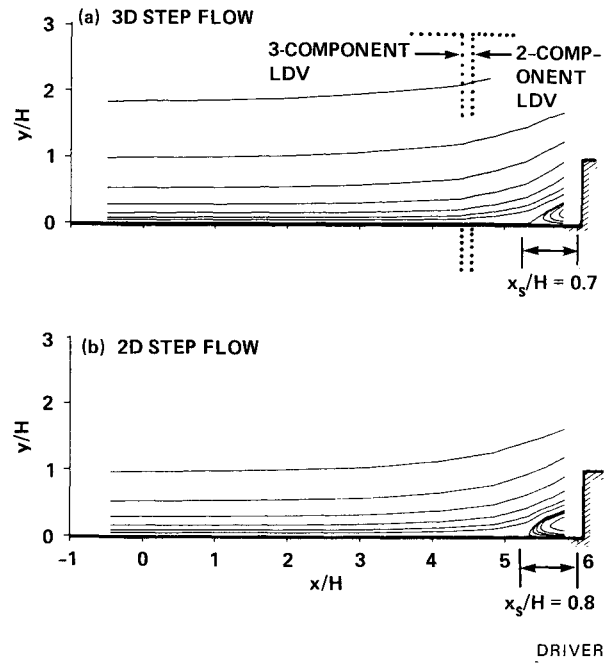

Fig. 2 Stream-function contours for forward-facing step flow.

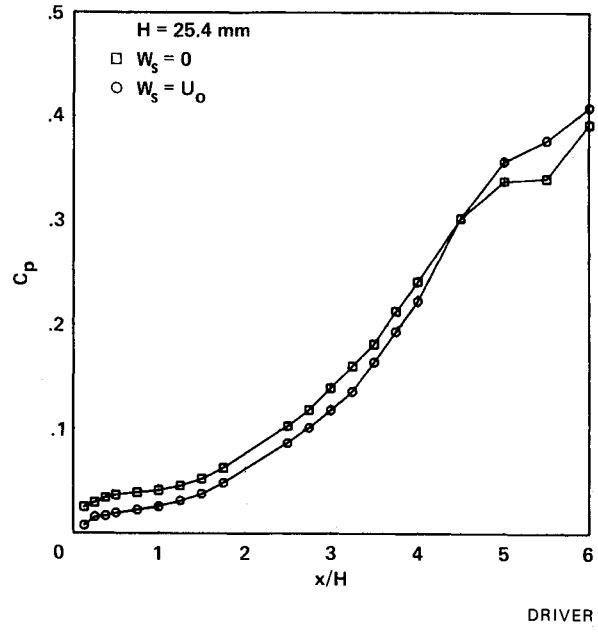

Fig. 3 Pressure distribution for forward-facing step flow.

nominally zero. Good axisymmetry was seen in the circumferential distributions of skin friction, and momentum balances were better than 7%. The flow was found to be essentially collateral at the end of the spinning section. For the case with the step, simple-integral momentum balances were not possible because of variations in static pressure in the normal direction which were not measured.

Test Cases

Four cases were studied:

1) Step with cylinder spinning ($W_s = U_o = 36.5$ m/s), referred to as three-dimensional step flow.

2) Step with cylinder stationary ($W_s = 0$ and $U_o = 36.5$ m/s), referred to as two-dimensional step flow.

3) Zero $\partial P/\partial x$ with cylinder spinning ($W_s = U_o = 36.5$ m/s), referred to as three-dimensional flat-plate flow.

4) Zero $\partial P/\partial x$ with cylinder stationary ($W_s = 0$ and $U_o = 36.5$ m/s), referred to as two-dimensional flat-plate flow.

The two-dimensional step flow (without spin) experiences an extra rate of strain ($\partial U/\partial x$, due to pressure gradient) in addition to the usual rate of strain ($\partial U/\partial y$). The spinning case contains a combination of extra rates of strain caused by pressure gradient $\partial U/\partial x$, transverse shear $\partial W/\partial y$, and curvature W/r making the flow somewhat more challenging for turbulence models. In both flows, there could be some effect of longitudinal curvature. The third and fourth cases are repeat measurements of Driver and Hebbar's[2] zero pressure-gradient flow and are used for comparison purposes to assess the effect of $\partial U/\partial x$ strain rate.

Computations

Calculations were performed using a boundary-layer solver,[10] which assumes a uniform pressure distribution in the y direction. Pressure is prescribed in the calculations using the surface static pressure distribution from the experiment. The assumption that pressure is uniform in the y direction is not a good one for the step flow, but is tolerable in the inner layer of the boundary layer. This assumption was necessary because of the lack of a Navier–Stokes equation solver. The calculations employ a Launder et al.[11] Reynolds stress equation turbulence model.

Results and Discussion

Stream-function contours obtained from velocity measurements (Figs. 2a and 2b) show the general features of the forward-facing step flows. Flow divergence from the wall is seen as far forward as 5 step heights ahead of the step. Boundary-layer detachment is seen at $0.7H$ ahead of the step in the spinning case (Fig. 2a) and $0.8H$ in the two-dimensional case (Fig. 2b). Both cases indicate that reattachment occurs on the face of the step. One difference between the two cases is the size and shape of the separation bubble; a thinner bubble is seen in the case with spin. This difference in the relative size of the bubbles is not believed to be due to transverse strain effects, but rather to a difference in the upstream U-velocity distribution. Stream-function contours appear quite smooth, even at the interface between three-dimensional and two-dimensional LDV measurement stations (at $X/H = 4.4$ and 4.5, respectively) shown in Fig. 2a, indicating good self-consistency of the data. Measurements at 14 streamwise stations were used to determine the stream-function contours for the three-dimensional step, and 10 stations were used in the two-dimensional step flow.

Surface pressure (Fig. 3) is seen to increase rapidly with proximity to the step. There are only slight differences between the case with spin and that without. Normal pressure gradients exist in this flow and pressure is not uniform through the boundary layer. At distances further from the wall, the pressure distribution will look different.

Flowfield Measurements

Velocity measurements of the three-dimensional spinning cases with and without pressure gradients are shown in Fig. 4a for a location $1.66H$ upstream of the step ($0.96H$ upstream of separation). The effect of pressure gradient is clearly seen to retard the streamwise velocities, while the transverse velocity appears to be only negligibly affected by the streamwise pressure gradient.

Shear stresses (Fig. 4b) appear to be unaffected by the pressure gradient at this location. The minimal differences are an indication of the inability of the turbulence to react to the rapid application of $\partial U/\partial x$ strain. Perhaps the most striking feature is the local minimum in $\overline{uv}$ shear stress seen 0.2δ from the wall in both zero and adverse pressure-gradient cases. Two-component LDV measurements were performed further

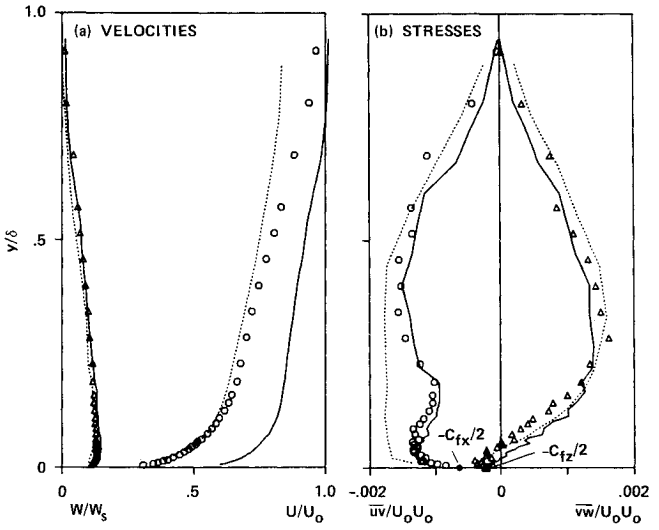

Fig. 4 Three-dimensional forward-step velocity and stressed at $X/H = 4.4$: $--\ \partial P/\partial X = 0$; ○, △ $\partial P/\partial X > 0$ measurements; ... $\partial P/\partial X > 0$ calculations.

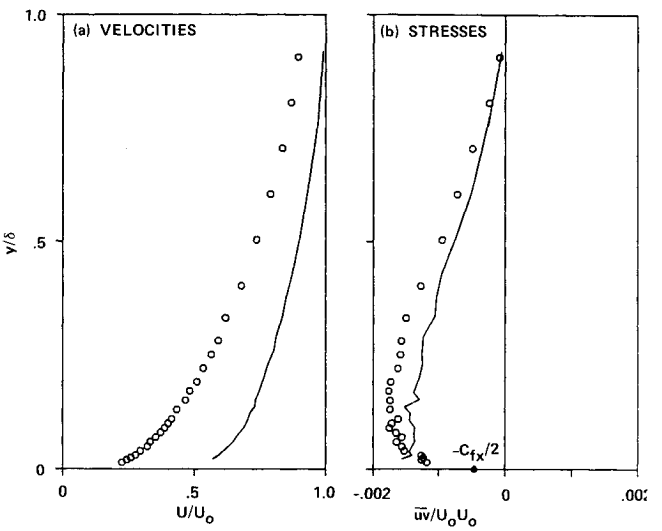

Fig. 5 Two-dimensional forward-step velocity and stresses at $X/H = 4.5$; ○ $\partial P/\partial X > 0$; $--\ \partial P/\partial X = 0$ measurements.

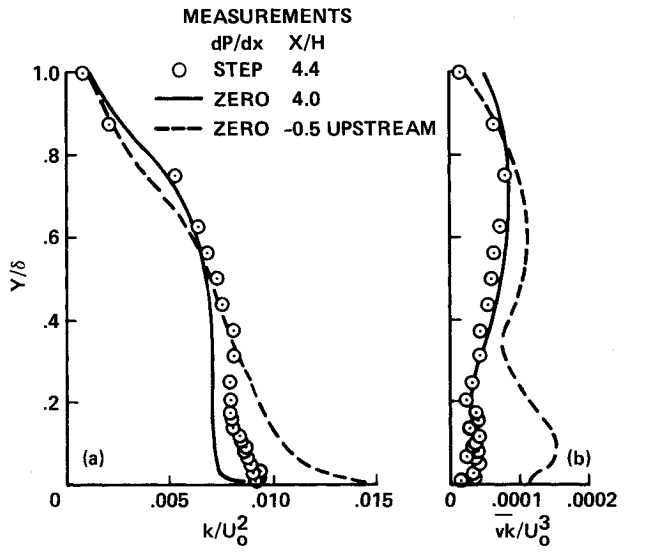

Fig. 6 Kinetic energy and velocity triple correlation measurements for the spinning case.

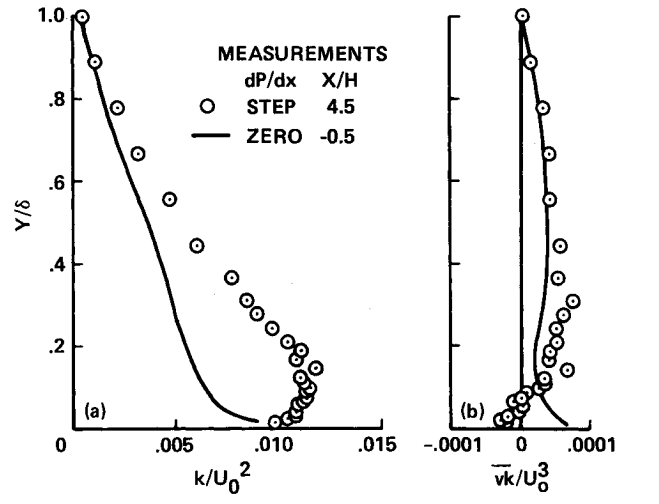

Fig. 7 Kinetic energy and velocity triple correlation measurements for the nonspinning case.

downstream where three-component measurements were not possible (due to optical restraints), and this local minimum was seen to persist downstream. Similarly, Bradshaw and Pontikos[1] saw a global reduction of shear stress (rather than local) in their "infinite" swept wing flow; they associated this reduction with transverse strain effects. Some of the reduction seen here is probably due to transverse strain effects, but also the shear stress is reduced as a result of the flow adjusting to a new wall boundary condition ($W_s = 0$) which carries a lower level of turbulence production associated with $\partial W/\partial y$.

The corresponding two-dimensional step flow (seen in Fig. 5b) did not exhibit a local minimum in Reynolds shear stress, instead a local maximum is seen (typical of two-dimensional adverse pressure-gradient flows[3]). The velocity distribution in the two-dimensional step case (Fig. 5a) for a location $1.56H$ ahead of the step shows a larger velocity deficit than that seen in the corresponding three-dimensional step flow. Differences between the two-dimensional and three-dimensional streamwise velocity profiles originate upstream in the zero pressure-gradient region of the flow. Higher velocities near the wall in the three-dimensional spinning case are a result of destabilizing curvature which enhances mixing and momentum transfer between the wall and freestream (see Appendix).

Calculations of the time-averaged velocity field for the pressure-gradient case, shown in Fig. 4a, compare well with the measurements in the near-wall region. Away from the wall, lower velocities are predicted because of the solver's lack of a normal momentum equation and the erroneous assumption that normal pressure gradient is zero. Comparisons between the measurements and the calculations should be limited to the inner portion of the boundary layer for this reason.

Calculations of the streamwise component of Reynolds shear stress, seen in Fig. 4b, fail to predict the local minimum in shear stress seen in the experiment. Again, this local minimum is not peculiar to the step-induced pressure gradient, but is a characteristic of the relaxation process. To the authors' knowledge, none of the current turbulence models can predict this phenomenon.

Turbulent kinetic energy in the spinning case is lower downstream than it is on the upstream spinning section (see Fig. 6a), primarily due to a loss in w^2 production associated with the $\partial W/\partial y$ gradients. However, pressure gradient serves to increase the kinetic energy above the zero pressure-gradient levels as a result of increased $\partial U/\partial y$ gradients. The increase due to the pressure gradient for the non-spinning case is more

pronounced, due to yet steeper $\partial U/\partial y$ gradients (see Fig. 7a).

Diffusion of turbulent kinetic energy and thickening of the boundary layer is associated with the velocity triple correlations $\overline{vk}$ seen in Figs. 6b and 7b. Positive $\overline{vk}$ is an indication of kinetic-energy diffusion away from the wall, and negative $\overline{vk}$ indicates diffusion toward the wall. Triple product $\overline{vk}$ decays downstream in the spinning case, again primarily due to decay in $\overline{w^2}$ and $\overline{vw}$ once active on the spinning cylinder. Adverse pressure gradient only minimally effects $\overline{vk}$. In the no-spin case, $\overline{vk}$ adverse pressure gradient produces a change in sign (from positive to negative) near the wall, consistent with gradient diffusion-type modeling (see Fig. 7b). The magnitude of $\overline{vk}$ typically is assumed (modeled) to be proportional to the gradient of kinetic energy.

Momentum Balance

Turbulence modeling may not be important to the solution of the mean flowfield in many regions of the flow. One way to assess the importance of the turbulence model is to examine terms in the momentum balance.

Forward-facing step flows are overwhelmingly dominated by the pressure forces everywhere except very close to the wall as can be seen in Figs. 8a and 8b. Terms in the x-momentum equation

$$DU/Dt = -(1/\rho)\partial P/\partial x - r^{-1}\partial(r\overline{uw})/\partial r - \partial\overline{u^2}/\partial x$$

are plotted as a function of distance from the wall, where $(1/\rho)\partial P/\partial x$ is inferred from the balance. Here streamwise momentum loss, in both the three-dimensional and two-dimensional step flow, is almost exclusively a result of streamwise pressure gradient. Shear stress gradients are not significant until within $0.03H$ of the wall ($y^+ < 40$). It would appear that the shear stress gradient associated with the local minimum in shear stress distribution has little or no effect on the mean flow. The normal stress gradient ($-\partial\overline{u^2}/\partial x$) contributes to further decelerate the fluid (u^2, turbulent energy, increases at the expense of U^2 mean flow energy). It is encouraging to see that pressure gradient inferred from the balance of the momentum equation extrapolates nicely to the measured wall value of streamwise pressure gradient, shown with an arrow on Figs. 8a and 8b. The location shown $1.56H$ upstream of the step) represents the region of peak adverse pressure gradient, and subsequent profiles both upstream and downstream show somewhat milder gradients.

Cross-flow momentum is balanced solely by the transverse shear stress as seen in Fig. 9. Terms in the crossflow momentum equation which are nonzero are

$$DW/Dt + VW/r = -r^{-2}\partial(r^2\overline{vw})/\partial r$$

Away from the wall, the transverse flow experiences acceleration due to residual Reynolds shear stress forces which were created upstream by the spinning cylinder. While near the wall, transverse momentum is lost because of Reynolds shear stresses generated by the stationary wall. Uncertainties in the estimates of momentum loss are relatively large due to the minute size of the terms (10% of the size of streamwise momentum terms).

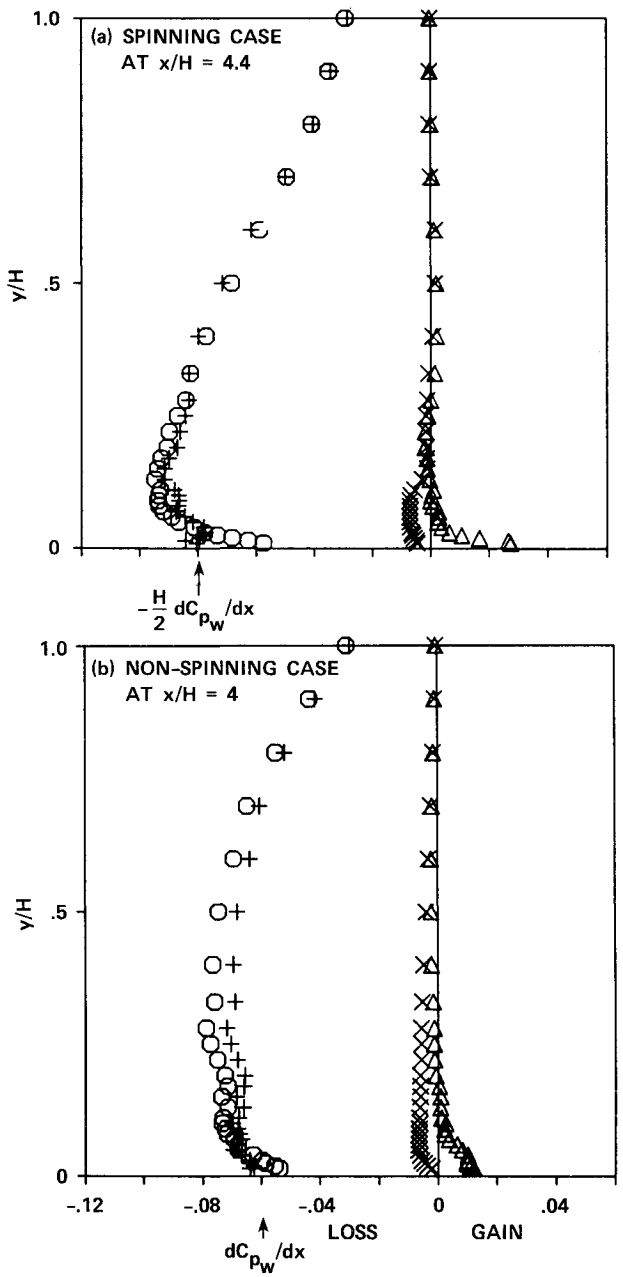

Fig. 8 The U-momentum equation balance; a) three-dimensional step flow at $X/H = 4.4$; b) two-dimensional step flow at $X/H = 4.5$; ○$(DU/Dt)H/U_o^2$; + $(-\frac{1}{\rho}\partial P/\partial x)H/U_o^2$; △ $(-r^{-1}\partial r\overline{uv}/\partial r)H/U_o^2$; × $(-\partial\overline{u^2}/\partial x)H/U_o^2$.

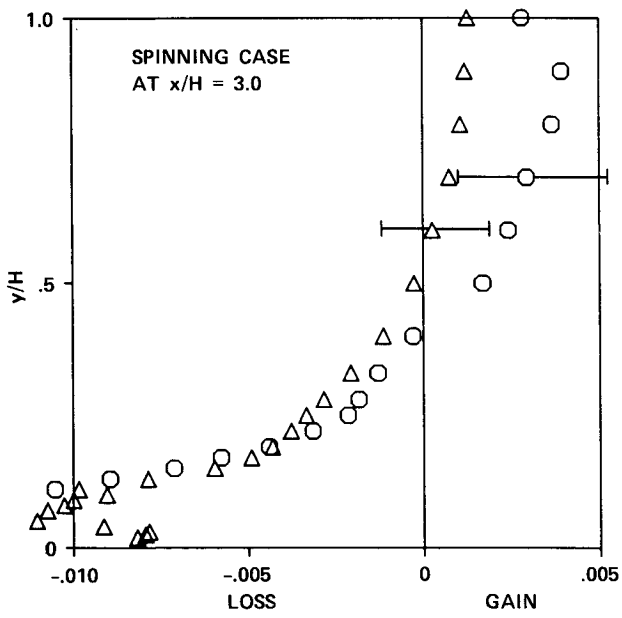

Fig. 9 The W-momentum equation balance for three-dimensional step flow at $X/H = 3.0$: ○ $(DW/Dt + VW/r)H/U_o^2$; △$(-r^{-2}\partial r^2\overline{uw}/\partial r)H/U_o^2$.

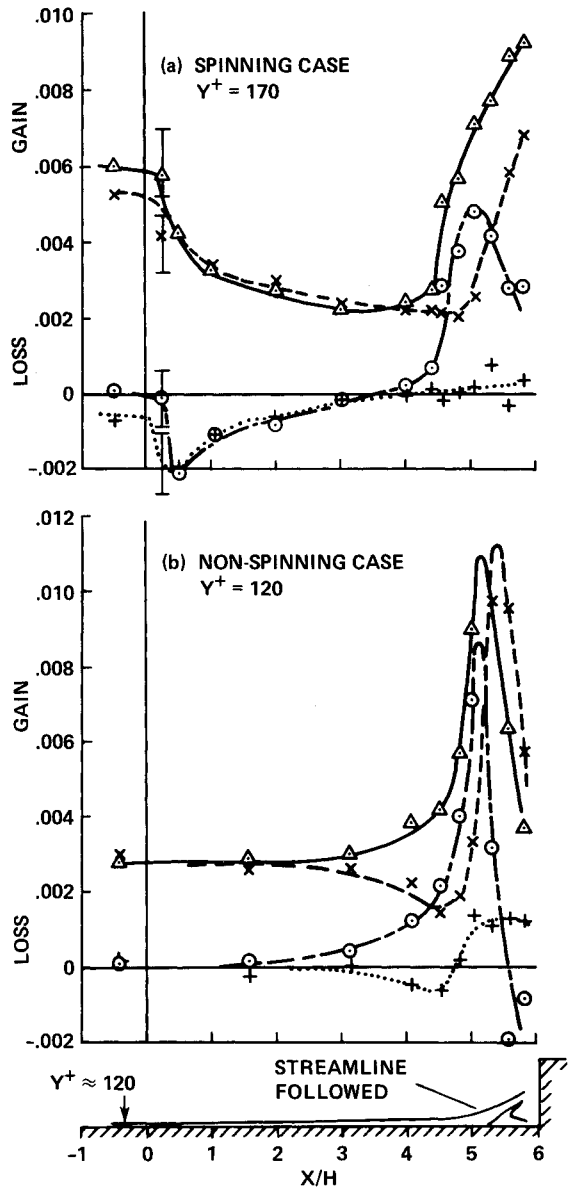

Fig. 10 Kinetic-energy equation balance along a streamline: a) three-dimensional step flow; b) two-dimensional step flow: △ (production)H/U_o^3; ○ (Dk/Dt)H/U_o^3; + (diffusion)H/U_o^3; × (−dissipation)H/U_o^3.

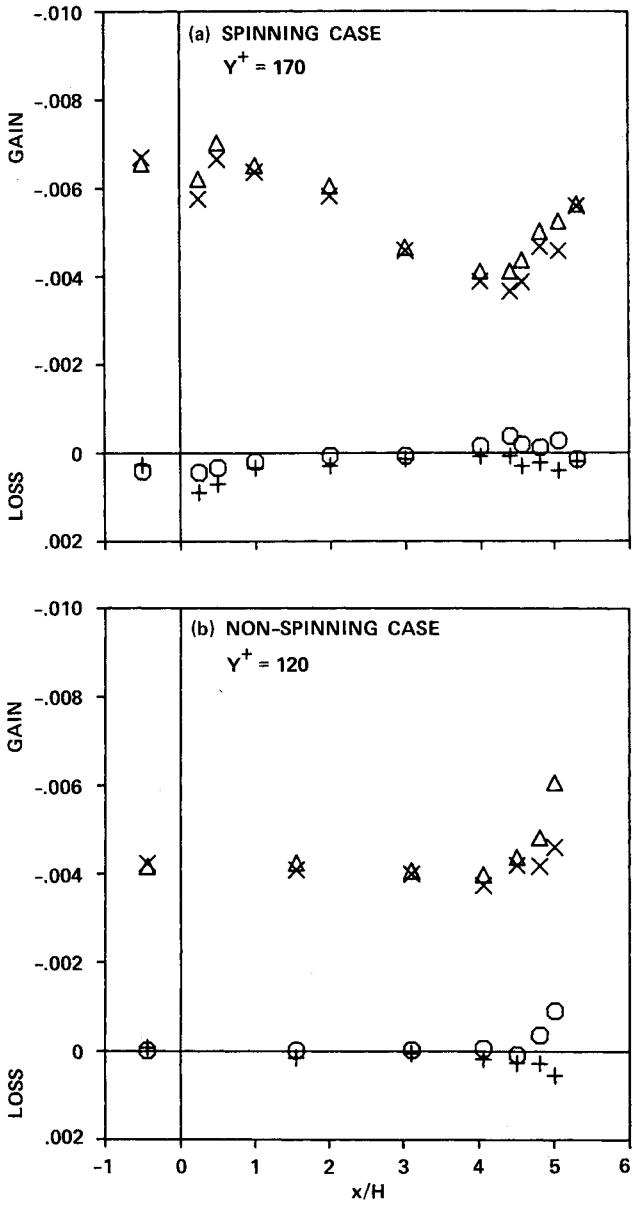

Fig. 11 The $\overline{uv}$ equation balance along a streamline: a) three-dimensional step flow; b) two-dimensional step flow: △ (production)H/U_o^3; ○ (D$\overline{uv}$/D$t - \overline{uw}W/r$)H/U_o^3; + (diffusion)H/U_o^3; × (−pressure strain + ε_{uv})H/U_o^3.

Kinetic-Energy Balance

Many turbulence models require a solution to the turbulent kinetic-energy equation in the process of modeling the Reynolds stresses. Although the equation can be derived from first principles, some of the terms in it involve new variables which require further modeling. Nevertheless, the hope is that modeling the terms in the kinetic-energy equation is easier (more universal) than modeling the kinetic energy itself.

Turbulent kinetic-energy balances were performed on both the two-dimensional and three-dimensional forward-step cases.

$$\underbrace{Dk/Dt}_{\text{convection}} = \underbrace{[-r^{-1}\partial(r\overline{vk})/\partial r - \partial\overline{uk}/\partial x]}_{\text{diffusion}} - \underbrace{\varepsilon}_{\text{dissipation}}$$

$$+\underbrace{[-\overline{uv}\partial U/\partial r - \overline{vw}(\partial W/\partial r - W/r) - (\overline{u^2} - \overline{v^2})\partial U/\partial x]}_{\text{production}}$$

All terms in the kinetic-energy equation can be directly computed from the data with the exception of dissipation rate. Dissipation is therefore inferred from the balance of the equation. Terms in the equation were evaluated along a path of constant stream function (streamline in two-dimensional case) which originates in the log layer (y = 1.27 mm) upstream of the step, see Figs. 10a and 10b. The stream line followed (also shown in Fig. 10) narrowly skirts the separation bubble, and essentially passes through the outer edge of the shear layer defining the separation zone.

Upstream, in the unperturbed boundary layer, the production of kinetic energy is virtually equal to the dissipation rate with convection and turbulent diffusion nearly zero. This is expected for an equilibrium boundary layer under zero pressure-gradient conditions.

The production rate in the three-dimensional step flow is significantly higher than that of the two-dimensional step—this is due to the extra rate of strain from transverse flow, which contributes up to half of the total production. Downstream on the stationary section, where transverse strain has diminished, the production rate decreases to a level comparable to that for the two-dimensional case. Eventually, far enough downstream (where the pressure gradient has significantly modified the mean flow), rates of kinetic-energy pro-

duction increase. Part of this increase in production is due to the steep velocity gradients ($\partial U/\partial y$) created by an accelerating freestream and decelerating inner flow. Also, longitudinal flow curvature (associated with vertical flow) can add to flow instability and turbulent production. A flat-plate adverse pressure-gradient flow like Simpsons[3] does not experience an accelerating freestream, nor any significant longitudinal curvature. The calculations lack these two effects and consequently are not shown here. The $-(u^2-v^2)\partial U/\partial x$ term is not negligible and contributes up to 10% of the production in the vicinity of the separation.

Although production increases through the pressure gradient, dissipation initially stays constant (even decreases) before eventually increasing—the imbalance results in an increase in turbulent convection. Diffusion of kinetic energy, although small relative to production, is significant compared to convection. Large streamwise gradients of $\overline{uk}$ contributed significantly to the the diffusion term near separation (often equal in magnitude to gradients of $\overline{vk}$).

Reynolds Stress Equation Balance

Increasingly popular, Reynolds stress equation models involve solving partial differential equations for the individual components of Reynolds stress. These equations, although derivable from first principles, require modeling of many of the terms in the equation. This level of modeling is often needed in nonequilibrium flows where the evolution of Reynolds stress is slow relative to the evolution of the mean flow strain-rate.

Reynolds stress equation balances were performed on both the two-dimensional and three-dimensional forward-step cases. All terms in the Reynolds stress equation can be directly computed from the data with the exception of pressure–strain and dissipation rate of $\overline{uv}$.

$$\underbrace{\mathrm{D}\overline{uv}/\mathrm{D}t - \overline{uw}W/r}_{\text{convection}} = \underbrace{-r^{-1}\partial(\overline{ruv^2})/\partial r - \partial\overline{vu^2}/\partial x + \overline{uw^2}/r}_{\text{diffusion}}$$
$$+\underbrace{(-\overline{v^2}\partial U/\partial y + \overline{uw}W/r)}_{\text{production}} + \underbrace{\phi_{uv}}_{\text{pressure-strain}} - \underbrace{\varepsilon_{uv}}_{\text{dissipation}}$$

These unmeasurable terms, pressure-strain and dissipation of uv, are lumped together and inferred from the balance of the equation. Dissipation of $\overline{uv}$ stress (ε_{uv}) is believed to be small and this lumped sum will be referred to as the pressure-strain. Like the kinetic-energy equation, terms in the $-\overline{uv}$ stress equations were evaluated along the same path of constant stream function as that for the kinetic-energy equation (originating at $y = 1.27$ mm, see Figs. 11a and 11b).

The three-dimensional forward-step flow case (Fig. 11a) exhibits a drop in Reynolds stress production initially, before ultimately increasing in the pressure-gradient region downstream. This initial drop comes as result of a drop in v^2 stress. Convection of $\overline{uv}$ stress, by comparison, is extremely small; likewise, diffusion of $\overline{uv}$ is also very small. The pressure-strain (plus dissipation), which requires modeling, is almost exclusively balancing the production term. The small relative size of the convective term (for which the model equation is solved) could make it difficult to design a pressure-strain model which will accurately predict the observed drop in $\overline{uv}$ stress associated with transverse strain.

The two-dimensional forward-step flow (Fig. 11b) exhibits no initial drop in production as did the three-dimensional case. Otherwise, the two cases are very similar in nature. Convection appears a little larger in the two-dimensional case than in three-dimensional case.

Balance of the $\overline{vw}$ stress equation given by

$$\underbrace{\mathrm{D}\overline{vw}/\mathrm{D}t - (\overline{w^2}-\overline{v^2})W/r}_{\text{convection}}$$
$$= +\underbrace{(-r^{-1}\partial(\overline{rwv^2})/\partial r - \partial\overline{uvw}/\partial x - (\overline{wv^2}-\overline{w^3})/r)}_{\text{diffusion}}$$
$$+\underbrace{(-\overline{v^2}\partial W/\partial r + \overline{vw}W/r)}_{\text{production}} + \underbrace{\phi_{vw}}_{\text{pressure-strain}} - \underbrace{\varepsilon_{vw}}_{\text{dissipation}}$$

for the three-dimensional forward-step case is shown in Fig. 12. Production of $\overline{vw}$ stress, the largest term in the equation, is seen to decay with distance downstream of the spinning cylinder. This drop in production corresponds to the absence

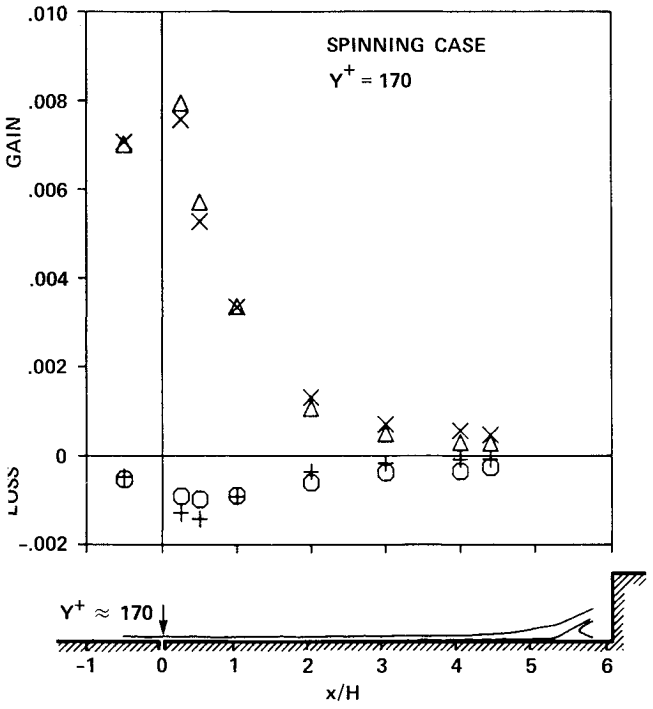

Fig. 12 The $\overline{vw}$ equation balance along a streamline for three-dimensional step flow: △ (production) H/U_o^3; ○ $[\mathrm{D}\overline{vw}/\mathrm{D}t - (w^2-v^2)\mathrm{W}/\cdot]H/U_o^3$; + (diffusion) H/U_o^3; × (−pressure-strain + ϵ_{vw}) H/U_o^3.

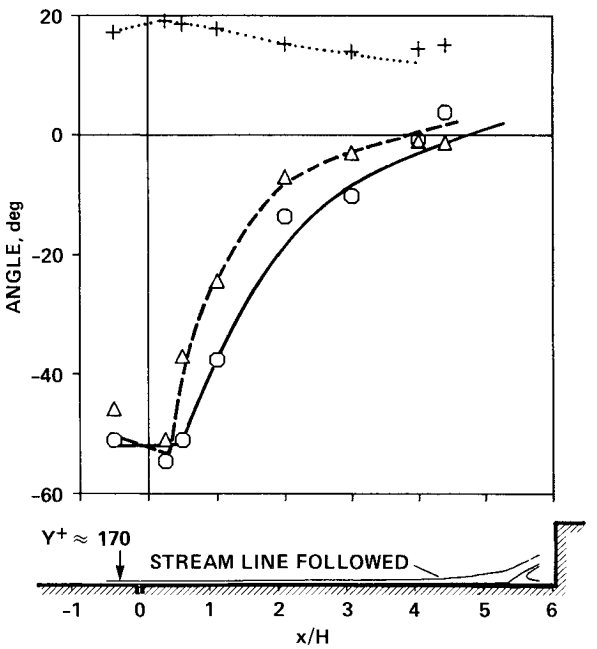

Fig. 13 Strain rate and stress directions: $\partial P/\partial X > 0$; ○ $\tan^{-1}(-\overline{vw}/-\overline{uv})$; △ $\tan^{-1}[(\partial W/\partial r - W/r)/(\partial U/\partial y)]$; +flow angle; $\partial P/\partial X = 0$; —— $\tan^{-1}(-\overline{vw}/-\overline{uv})$; - - - $\tan^{-1}[(\partial W/\partial r - W/r)/(\partial U/\partial y)]$, . . . flow angle.

of spin and, therefore, $\partial W/\partial y$ gradients. Pressure-strain likewise drops along with production. Convection is negative indicating a net decay of $\overline{vw}$ stress with distance along the streamline. Unlike the $\overline{uv}$ stress equation, convection of $\overline{vw}$ stress is relatively large compared to production, providing more leeway for error in modeling the pressure-strain term. Negative diffusion indicates that there is a net outflow of $\overline{vw}$ stress away from this streamline via turbulent mixing.

Turbulence Lag Phenomenon

One frequently used assumption in turbulence modeling is the Boussinesq approximation (stress proportional to mean flow strain rate). The assumption borrowed from laminar flow theory requires specifying a constant of proportionality which depends on the turbulence and may vary with location in the flow.

In order for the assumption to work, the mean flow strain-rate direction has to be equal to the shear-stress direction. A measure of the mean flow strain-rate direction and the shear-stress direction is shown in Fig. 13 for flow along a streamline originating upstream at $y = 1.27$ mm ($y^+ = 170$). Upstream, the stress and strain-rate directions are nearly equal (-50 deg), but soon after the cessation of spin the strain rate turns to align with the tunnel axis (0 deg). Delayed by about one boundary-layer thickness, the stress direction turns to align with the strain. This difference between the stress and the strain-rate directions (as much as 15 deg) is characteristic of three-dimensional boundary layers and is not accounted for in the Boussinesq approximation.

Differences between the zero pressure-gradient case and step-induced pressure-gradient case are insignificant up to $X = 4H$. Beyond $X = 4H$, the flow angle for the pressure-gradient case starts to increase. Although the direction of the strain rate is virtually the same for the two cases, the stress-vector direction does differ slightly. Interestingly, in the case of pressure gradient, the stress vector overshoots the strain-rate direction. This overshoot phenomenon seems to be confined to the region near the wall; further out in the flow, the stress-vector direction is always more negative than the strain-rate direction. A similar overshoot of sorts was seen in Johnston's "swept forward-facing step"[5] flow in which the stress-vector was seen to turn in a direction opposite to that of the strain-rate direction. This is not understood, and experimental uncertainty cannot be ruled out.

Conclusions

In an effort to assess turbulence models, turbulence measurements have been carried out in two flows, one with crossflow strain and the other with both streamwise pressure gradient and crossflow strain.[12] Three components of velocity and all six Reynolds shear stresses were measured using a three-component laser Doppler velocimeter. Two cases were studied, one case with transverse flow and the other without. Both cases included streamwise pressure gradient.

The streamwise flow was shown to be predominantly pressure driven with viscous forces becoming important only very near the wall. The pressure rise was found to occur over such a short distance that turbulent stresses were barely able to respond before the flow separated.

Crossflow and transverse shear stress seem to be insensitive to streamwise pressure gradient, at least for this case of sudden pressure gradient.

Streamwise shear stress exhibits a local minimum in both the zero and adverse pressure-gradient flow, possibly due in part to transverse strain effects like those seen in the "infinite" swept wing of Bradshaw and Pontikos.[1] Calculations fail to predict this local minimum in shear stress.

Turbulent kinetic-energy production is seen to grow rapidly in the vicinity of the step, as a result of steep mean-flow gradients $\partial U/\partial y$ created by the accelerating external flow and decelerating inner flow. Dissipation (deduced by balance of the equation) grows less quickly than production and the imbalance leads to growth in kinetic energy.

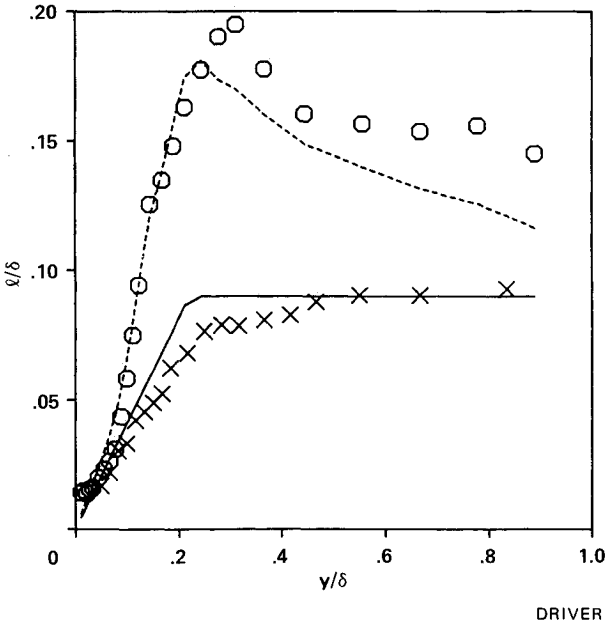

Fig. A.1 Mixing-length distribution in zero $\partial P/\partial X$ at $X/H = -0.5$; ○ with spin; × no spin; —— Prandtl mixing length (l_o); - - - $l = l_o(1 - 7Ri)$.

Reynolds stress equation balances were performed on the $\overline{uv}$ stress equation showing the small magnitude of the convective term relative to the pressure-strain term. This could make it difficult to design a pressure-strain model which will accurately predict the observed drop in $\overline{uv}$ stress.

The principal strain-rate direction was compared with the principal shear-stress direction, and as seen in other three-dimensional flows, the stress direction points in a different direction than the strain-rate vector by as much as 15 deg. Where the flow is collateral, the strain-rate direction and the stress direction are the same; but where the flow is relaxing, the stress direction lags in development behind the strain-rate direction. No significant differences in the lag rate were detected between the zero and adverse pressure-gradient cases.

Appendix

A measure of the destabilizing effect of rotation on the turbulence can be seen in a mixing-length formulation where

$$l = \sqrt[4]{uv^2 + vw^2}/\sqrt{(\partial U/\partial r)^2 + (\partial W/\partial r - W/r)^2}$$

In a two-dimensional flat-plate-type boundary layer, the mixing length appears to obey the usual $l_o = 0.41y$ scaling near the wall and $l_o = 0.09\delta$ away from the wall (see Fig. A.1). In the case with cylinder spinning, the l/δ distribution is larger and seems to obey the simple scaling reported by Bradshaw[13] in which $l = l_o(1 - 7Ri)$, where

$$Ri = 2(W/r)(\partial W/\partial r + W/r)/[(\partial U/\partial r)^2 + (\partial W/\partial r - W/r)^2]$$

Another, more physical way to understand the destabilizing effect of rotation is to consider a fluid blob (with transverse momentum ρW). The fluid's orbital path around the cylinder is maintained by an inward pressure force. If the fluid is perturbed from its original orbit to a new orbit further away (where inward pressure force is weaker and unable to hold the fluid in orbit), the fluid will now travel a path which diverges from the cylinder. This essentially contributes to a thickening of the boundary layer. Conversely, fluid which is bumped inward toward the center of rotation would be further drawn inward by pressure gradient (which increases with proximity to the wall).

Acknowledgment

We would like to express our sincere thanks to Drs. J. G. Marvin and M. Rubesin for their encouragement and suggestions during this investigation. This research was started while the second author held a senior National Council Research Associateship at the NASA Ames Research Center, and continued under a NASA-Ames University Consortium Agreement (Joint Research Interchange NCA2-127) while he was a faculty member in the Department of Aerospace Science Engineering, Tuskegee University, Tuskegee, Alabama.

References

[1]Bradshaw, P. and Pontikos, N., "Measurements in the Turbulent Boundary Layer on an 'Infinite' Swept Wing," *Journal of Fluid Mechanics*, Vol. 159, Oct. 1985, pp. 105–130.

[2]Driver, D. M. and Hebbar, S. K., "Experimental Study of a Three-Dimensional, Shear-Driven, Turbulent Boundary Layer," *AIAA Journal*, Vol. 25, Jan. 1987, pp. 35–42.

[3]Simpson, R., Chew, Y., and Shivaprasad, B., "The Structure of a Separating Turbulent Boundary Layer. Part 1. Mean Flow and Reynolds Stresses," *Journal of Fluid Mechanics*, Vol. 113, Dec. 1981, pp. 23–51.

[4]Elsenaar, A., Van den Berg, B., and Lindhout, J., "Three-Dimensional Separation of Incompressible Turbulent Boundary Layer on an Infinite Swept Wing," *Flow Separation*, AGARD CP-168, 1975.

[5]Johnston, J., "Measurements in a Three-Dimensional Turbulent Boundary Layer Induced by a Swept, Forward-Facing Step," *Journal of Fluid Mechanics*, Vol. 42, Part. 4, May 1970, pp. 823–844.

[6]Anderson, S. and Eaton, J., "An Experimental Investigation of Pressure-Driven Three-Dimensional Turbulent Boundary Layers," Thermosciences Div., Dept. of Mechanical Engineering, Stanford Univ., Stanford, CA, Rept. MD-49, June 1987.

[7]Furuya, Y., Nakamura, I., Yamashita, S., and Ishii, T., "Experimental Investigation of the Relatively Thick Turbulent Boundary Layers on a Rotating Cylinder in Axial Flows (2nd Rept., Flows under Pressure Gradients)", *Bulletin of the Japan Society of Mechanical Engineers*, Vol. 20, No. 140, Feb. 1977, pp. 191–200.

[8]Hebbar, S. K. and Driver, D. M., "Experimental Investigation of a Swirling, Axisymmetric, Turbulent Boundary Layer with Pressure Gradient," *AIAA Journal*. Vol. 25, April 1987, pp. 521–522.

[9]Driver, D. M. and Hebbar, S. K., "Experimental Study of a Three-Dimensional, Shear-Driven, Turbulent Boundary Layer Using a Three-Dimensional Laser Doppler Velocimeter," AIAA Paper 85-1610, July 1985.

[10]Wilcox, D. C., "Recent Improvements to the Spinning Body Version of the EDDYBL Computer Program," DCW Industries Inc., Studio City, CA, Rept. DCW-R-24-01, Nov. 1979.

[11]Launder, B., Reece, G., and Rodi, W., "Progress in the Development of a Reynolds-Stress Turbulence Closure," *Journal of Fluid Mechanics*, Vol. 68, Part. 3, April 1975, pp. 537–566.

[12]Driver, D. M. and Hebbar, S. K., "Three-Dimensional, Shear-Driven Boundary-Layer Flow with Streamwise Adverse Pressure Gradient—Data Report," NASA TM, to be published.

[13]Bradshaw, P., "Effects of Streamline Curvature on Turbulent Flow," NATO, AGARDograph No. 169, Aug. 1983.